

UC San Diego

UC San Diego Previously Published Works

Title

Insulated conducting cantilevered nanotips and two-chamber recording system for high resolution ion sensing AFM.

Permalink

<https://escholarship.org/uc/item/8gk363jf>

Journal

Scientific reports, 4(1)

ISSN

2045-2322

Authors

Meckes, Brian
Arce, Fernando Teran
Connelly, Laura S
et al.

Publication Date

2014-03-01

DOI

10.1038/srep04454

Peer reviewed



OPEN

SUBJECT AREAS:

ATOMIC FORCE
MICROSCOPY

IMAGING TECHNIQUES

Insulated Conducting Cantilevered Nanotips and Two-Chamber Recording System for High Resolution Ion Sensing AFM

Received
13 January 2014Accepted
4 March 2014Published
25 March 2014Brian Meckes¹, Fernando Teran Arce^{1,2}, Laura S. Connelly^{2,3} & Ratnesh Lal^{1,2,3}¹Department of Bioengineering, University of California, San Diego, La Jolla, CA 92093, USA, ²Department of Aerospace and Mechanical Engineering, University of California, San Diego, La Jolla, CA 92093, USA, ³Materials Science and Engineering Program, University of California, San Diego, La Jolla, CA 92093.Correspondence and
requests for materials
should be addressed to
R.L. (rlal@ucsd.edu)

Biological membranes contain ion channels, which are nanoscale pores allowing controlled ionic transport and mediating key biological functions underlying normal/abnormal living. Synthetic membranes with defined pores are being developed to control various processes, including filtration of pollutants, charge transport for energy storage, and separation of fluids and molecules. Although ionic transport (currents) can be measured with single channel resolution, imaging their structure and ionic currents simultaneously is difficult. Atomic force microscopy enables high resolution imaging of nanoscale structures and can be modified to measure ionic currents simultaneously. Moreover, the ionic currents can also be used to image structures. A simple method for fabricating conducting AFM cantilevers to image pore structures at high resolution is reported. Tungsten microwires with nanoscale tips are insulated except at the apex. This allows simultaneous imaging via cantilever deflections in normal AFM force feedback mode as well as measuring localized ionic currents. These novel probes measure ionic currents as small as picoampere while providing nanoscale spatial resolution surface topography and is suitable for measuring ionic currents and conductance of biological ion channels.

Nanoscale transport of ionic species plays an essential role in determining the properties of biological as well as synthetic systems. In biological systems, ionic currents are primarily transported through the controlled activity of membrane pores called ion channels. Currently, ionic currents through individual channels are measured with the patch clamp technique and the 3D structures are imaged with EM, X-ray diffraction, and AFM. However, there is no technique available for simultaneous study of single channel structure and activity. Atomic force microscopy¹ (AFM) allows high resolution 3D imaging using the probe-sample interaction force as a feedback signal. Scanning ion conductance microscopy (SICM), a variant of AFM, allows high resolution microscopy utilizing ionic current between a conducting probe and a reference electrode as the feedback signal². Scanning electrochemical microscopy (SECM), another variation of AFM, uses electrochemical current gradients for positioning³. All of these imaging modalities allow for non-contact, non-destructive structural imaging and measurement of the localized currents in fluid, a necessity for studying native biological systems, including ion channels and receptors^{4–9}.

SICM and SECM usually do not have the force feedback control of an AFM. In order to image the surface topography of, and the currents through, an ion channel, SICM was originally combined with AFM to study porous membrane topography with force feedback modes of AFM, while simultaneously measuring the ionic current passing through the micro-porous membrane^{10,11}. This approach was further expanded for the study of the transport of electrochemically active species through pores while measuring the membrane structure^{12–14}. In this combined AFM-SICM, the probes utilized were created from glass pipettes that allowed localized ionic current measurements. However, the size of the pipette-tip was too large (>30 nm) to provide single channel resolution. For high resolution ionic current measurement and 3D imaging, the cantilever probes require a nanoscale conducting tip apex while the remainder of the probe is fully insulated from ions, such as in insulated wires^{12,15}, and microfabricated probes^{13,16,17}. Wire cantilevers offer the benefit of simple fabrication compared to microfabricated or glass pipette AFM cantilevers. Tungsten wires have been utilized in extracellular as well as intracellular neural recording and STM imaging due to their strength and electrochemical properties that allow

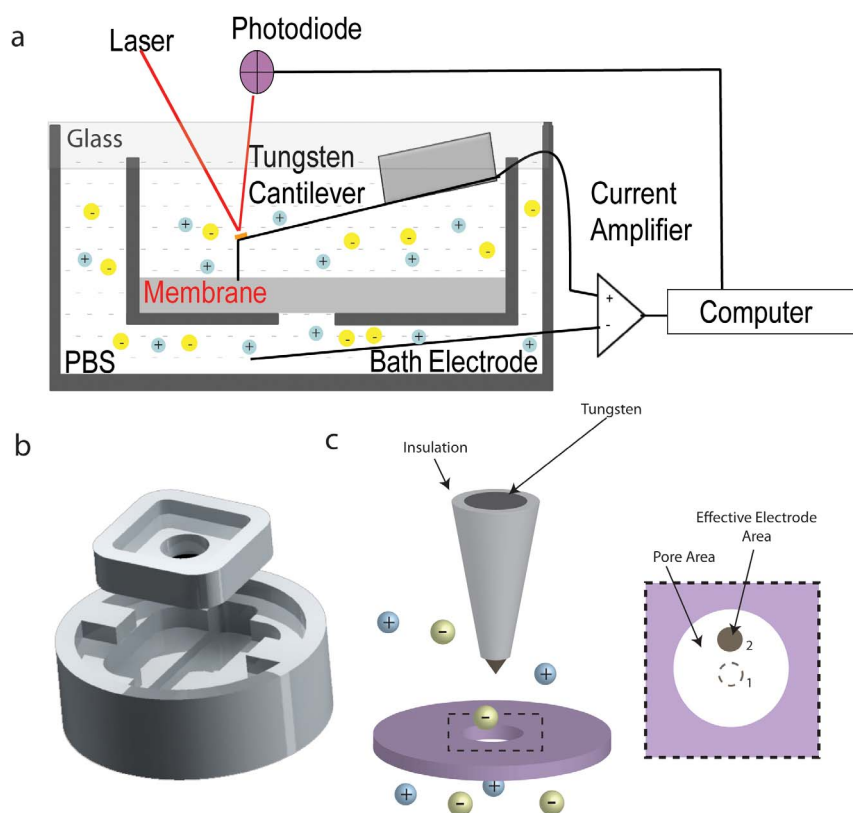


Figure 1 | Schematic of the setup used for imaging the surface topography and ionic current. (a) The ionic currents are measured with a conducting tungsten cantilever probe. A Ag/AgCl bath electrode acts as the counter electrode that is electrically separated from the tungsten probe by a membrane. The current measured between the two electrodes is passed through a current amplifier to the AFM controller. (b) The two chamber AFM system for imaging ionic currents passing through membranes. (c) Schematic of the probe over a pore. The effective electrode area determines the probe conduction behavior when the exposed area near the tip apex is smaller than the pore diameter.

for fine etching of the tip^{18,19}. Significantly, tungsten wire electrodes insulated with non-conducting coating except for 3–5 micrometer of the conducting tip, called Solid-Conductor Intracellular NanoElectrodes (SCINs), have been used to record intracellular neuronal action potential (AP) as well as subthreshold currents with 10 kHz temporal resolution²⁰. However, the large conducting region of the wire electrodes reduces its electrical current sensitivity – currently available wire electrodes measure currents too large for recording single ion channel current and conductance which is usually in picoamperes (pA) for biologically relevant potential difference.

Here, we present a simplified method for fabrication of tungsten wire AFM probes capable of high resolution imaging of the structure of, and very low (pA) ionic currents through pores. These tungsten probes were coated with non-conducting materials except for a nanoscale area on probe apex in order to record small ionic currents flowing through the pores. In addition, we also designed a two chamber electrical recording and molecular transport system for imaging currents passing through micro- and nano-porous membranes. Topography of 20 nm pores was successfully imaged while simultaneously measuring localized pA currents using this system. This approach allows for probes that can be integrated with any AFM system for high resolution structure-activity imaging of biomolecules.

Results

Cantilever Fabrication and Device Set up. Etched sharp tungsten wires (15 cm length) coated in epoxylite were attached to custom steel chips (1.6 mm × 2 mm) such that 2–3 mm of the wire, the sharpened end, extended off the front edge of the chip. The blunt end of the wire was used to form an electrical connection to relay

feedback signal to the AFM. The sharp end of the wire was bent at 75° such that the tip pointed downward. The wires were subsequently further insulated in electrophoretic paint to fill in gaps in the insulation while maintaining the exposed tip apex (Fig. 1 c). Gold mirrors were fixed to the end of the cantilever (as described in methods) to allow for optical detection of cantilever deflection in AFM imaging (Fig. 1 a). A custom built two chamber AFM setup was configured for imaging ionic currents across a porous aluminum oxide membrane (Fig. 1 a,b) where the tungsten cantilever served as a working electrode in the top cup while a Ag/AgCl counter electrode was placed in the bottom cup. Ionic currents between the top and bottom chambers were imaged through membranes placed over a single hole connecting the two chambers. The tungsten wire probe was used with the fluid cell cantilever holder of our AFM, with the blunt end of the tungsten wire exposed and connected to a patch clamp amplifier to pass the currents to the AFM. Testing of the cantilevers found resonance frequencies between 3–7 kHz in fluid.

Principle of Operation. Principle of AFM force-feedback mode imaging is well described and relies simply on using the cantilever deflection (due to force-field interaction between the tungsten wire probe and sample) for controlling/measuring the probe-sample distance as the cantilever wire probe raster scans over the sample. For measuring the ionic current for feedback (SICM, SECM modes), the system operates by limiting the ionic currents that are able to access the exposed tip of the probe as the probe approaches the surface^{2,3,6}. The measured current is determined by the exposed area of the probe when at far distances from the surface. Small electrode areas lead to small currents (pA range). For imaging of



currents through pores (Fig. 1 c), the currents passing through the pore will be defined by the geometry of the pore and the thickness of the membrane. However, when the area of the working electrode (i.e. the probe) is much smaller than the pore, the measured ionic currents will be dominated by the exposed probe area as the current density through the probe will be much higher. The current observed over the pore will remain approximately the same for the entire area of the probe whether it is in the center of the probe or the periphery (Fig. 1 c). This is true for large pores ($>1\ \mu\text{m}$) and nanopores where the measured currents are small due to the electrode area being significantly less than the pore area.

Probe Characterization. I–V curves of fully-coated wire cantilevers were performed following wire mounting and reinsulation to characterize the quality of the probes. These measurements were performed when the probe was withdrawn to distances far above the surface ($>100\ \mu\text{m}$) to prevent inhibited ion transport currents seen with SICM probes². Currents were measured as the voltage was ramped at different rates across a 400 mV range. The measured ionic currents in phosphate buffered saline (PBS) were in the pA range indicating that only a small portion of the probe was not insulated (Fig. 2 a). Hysteresis in the curves was observed at greater voltage scanning rates. This is indicative of capacitance from incomplete sealing of the metal probe²¹.

I–V curves were also performed in the presence of the electrochemically active specie ferrocyanide ($\text{Fe}(\text{CN})_6^{4-}$). These voltage ramps were performed in a two-electrode setup to provide an estimate of the exposed area of the probe. I–V curves performed over a 1 V range (Fig. 2 b) show characteristic oxidation peaks. The area of the probes was estimated based on the steady-state currents observed using²²:

$$i_{lim} = 2\pi n F D C^* r_{app} \quad (1)$$

In this equation, i_{lim} is the observed steady-state oxidative/reductive current. n is the number of electrons transferred per a redox event. F is the Faraday constant. C^* is the bulk concentration of the active species, which was 100 mM. D is the diffusion coefficient ($6.7 \times 10^{-6}\ \text{cm}^2/\text{s}$). Measuring the steady state current allows for approximation of effective radius (r_{app}). From our measurements we found active radii ranging from 5–10 nm. This value likely overestimates the radii as it applies to the entire probe including any leakage not near the tip apex. It also includes currents generated from activity of tungsten.

Scanning electron microscopy (SEM) images of these probes used in the electrochemical measurements show features at the end of the tip in the nanoscale that are capable of obtaining high resolution images of the surface (Fig. 2 c). The gaps in the insulation utilized for electrical recording here, are not visible due their small size and the presence of a chromium coating utilized to image the probes in the SEM.

Ionic currents showed a dependence on the distance of the exposed cantilever probe tip from the surface. As the probe approaches the surface, the current begins to decrease due to reduced ionic access to the probe. This decrease occurs prior to deflection of the probe due to interaction with a mica surface (Fig. 2 d). Approach curves onto a track-etched polycarbonate membranes in non-porous regions show a similar decrease as those observed on the mica surface when utilizing a different probe with a different geometry. The retraction of the probe from the surface resulted in a recovery of the ionic current (Fig. 2 e). Observed hysteresis in these curves could be due to tip adhesion to the surface, as the retraction currents are reduced compared to the approach currents for the same height.

Structure and Ionic Current Imaging of Micro- and Nano-pores. Imaging of ionic currents through pores with simultaneous surface topography imaging was performed on synthetic porous membranes. Track-etched polycarbonate membranes with $0.8\ \mu\text{m}$ pores were

mounted in the two chamber AFM system. The tungsten wire cantilever was utilized to image the surface topography while simultaneously measuring the ionic current (Fig. 3 a–c). Ionic currents imaged over the pore increased by $\sim 3\ \text{pA}$ compared to when the probe was positioned over regions without pores. High correlation is observed between the pore locations in both modes of operation.

AFM imaging of the anodic aluminum oxide (AAO) membrane demonstrates pores on the order of 18 nm in height mode (Fig. 4). This is consistent with the expected pore diameters for the membrane. Current mode imaging, taken simultaneously with topographic imaging, confirms the presence of multiple pores in the membrane. The location and size of the pores are in the same location and of similar diameter in both concurrent imaging modes, confirming accurate reading. Scanning electron microscopy (SEM) images of the AAO membrane demonstrated similar structures to those imaged with the AFM (Supplementary Fig. S1).

Scanning ion conductance microscopy (SICM) was also performed with the tungsten wire cantilevers. This imaging mode used the ionic current as the feedback signal for z positioning of the probe since the observed current is dependent on the probe distance from the surface. Imaging of the AAO membranes in SICM mode resulted in structures similar to those observed with AFM and SEM (Supplementary Fig. S2). However, greater noise in this mode resulted in low resolution quality compared to the image using force feedback with ionic currents as the carry-along signal.

Discussion

Imaging of ionic currents through micro- and nano-porous samples requires a system that allows for highly localized current measurements while limiting leakage current bias. The use of electrophoretic paints for insulating sharp wires have been demonstrated to be an effective means to limit the conductive surface to the nanoscale^{12,13,23}, which is the technique we pursued. Two insulating coatings were used in the fabrication in this paper to 1) reduce the presence of cracks in the insulation and 2) allow the coating to get closer to the probe apex. Ionic currents measured by this probe were restricted to the pA ranges. This is indicative of successful insulation of the probes.

Imaging of the ionic currents on the AAO membrane show some overlap in the signal from multiple pores (Fig. 4). This occurs due to the close proximity of the pores to one another, as seen in SEM and AFM, and the size of the probe (Fig. 4 and S1). The ionic currents measured in this study are significantly smaller than the ionic currents passing through the porous membranes. For nanoscale pores, the currents would be in the nA to μA range. However, the observed currents are in the pA range. This occurs due to the restricted small electrode area for the ions to access (Fig. 1 c).

Extensive work has been performed in improving SICM probe resolutions to the nanoscale^{4,7,9,24}. However, combined SICM-AFM probes have been more limited. The tungsten probe presented here allows for simple fabrication of conducting probes such that only the tip apex remains conducting while being suitable for ion sensing AFM. The use of wire based cantilever probes for SPM has been previously reported for larger pores sizes of $600\ \text{nm}$ ¹³. However, the tungsten cantilevered probes reported here improve upon the resolutions of these previous SICM/SECM-AFM probes^{10,14,16} while reducing the complexity of fabrication.

Methods

Tungsten wires coated in Epoxylite with $40\ \mu\text{m}$ shafts etched over 5 mm were purchased from FHC (Bowdoin, ME). All experiments were performed in Dubecco's phosphate buffered saline obtained from Cellgro (Manassas, VA).

Probe Fabrication. Tungsten wires coated in Epoxylite were prepared and attached to a custom fabricated support chip with inert, non-water soluble Two Ton Epoxy (Devcon, Danvers, MA). The preinsulation of the wires along with the epoxy prevent currents from leaking from the wire to the steel support chip ($2\ \text{mm} \times 1\ \text{mm} \times 2\ \text{mm}$) (Figure 1A). The wires were attached such that the sharp end of the wire overhanging the edge of the support chip by 2.5 mm. After drying overnight, the wires

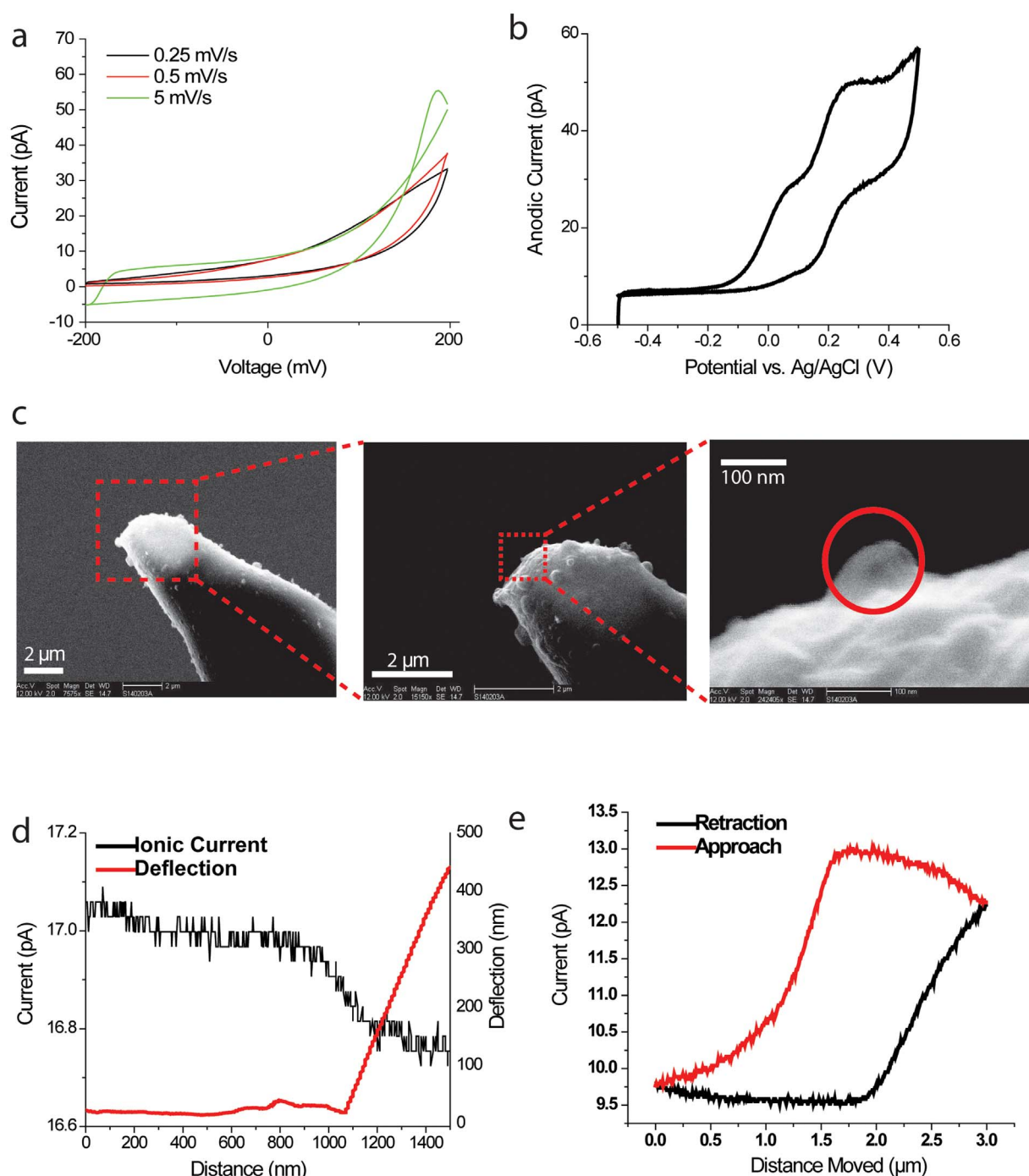


Figure 2 | Conducting properties of tungsten wire probes. (a) I–V curves a tungsten wire cantilevers in PBS. The voltages were ramped between ± 200 mV at rates of 0.25 mV/s, 0.5 mV/s, and 5 mV/s. (b) Cyclic voltammograms of the probe in the presence of 0.1 M $\text{Fe}(\text{CN})_6^{4-}$. An oxidation peak is observed near 0.2 V, not present in PBS. (c) SEM images of a tungsten cantilever probe at multiple scales. (d) Approach curve of tungsten electrode engaging a mica surface with both cantilever deflection and ionic current plotted. (e) Approach and retraction curves of a tungsten probe as it approaches a track etched polycarbonate membrane.

were bent with tweezers to create a tip for AFM imaging with a tip length of 0.5 mm creating a cantilever of 2 mm. The cantilevers were then reinsulated through three coatings with Clearclad electro-deposition paint (Clearclad Coating Inc, Harvey, IL). Each coating was performed with 30 s of deposition at 10 V followed by 20 min of baking at 160 °C with the tip pointing upward to prevent insulating the apex. Mirrors for laser detection in AFM were fabricated by sputtering gold onto a silicon substrate with a DC magnetron sputter to a thickness of 200 nm. Gold was then attached to the bend of the cantilever with a single drop of Two Ton Epoxy.

Two-chamber AFM Set up. A two-chamber AFM setup was designed and implemented for measuring electrical currents through porous membranes. The

two-chamber system consists of a bottom cup constructed from polycarbonate (Lexan) and a top cup (also polycarbonate) with a hole for ions to pass between the bottom cup to the top cup. A silver wire, electroplated with 1 M KCl at 1 V for 5 min, functioned as the Ag/AgCl reference electrode that was inserted into two-chamber AFM through a small hole in the bottom cup. Anodic aluminum oxide (AAO) membranes ($d_{\text{pore}} = 20$ nm) (Synkera, Longmont, CO) and track-etched polycarbonate filters ($d_{\text{pore}} = 0.8$ μm) (Whatman, UK) were used in imaging experiments. AAO membranes were fixed with vacuum grease to a silicon substrate with a 200 μm square pore (App Nano, CA). The silicon substrate with the membrane was attached with vacuum grease over the hole connecting the two-chambers and PBS was added above and below the membrane.

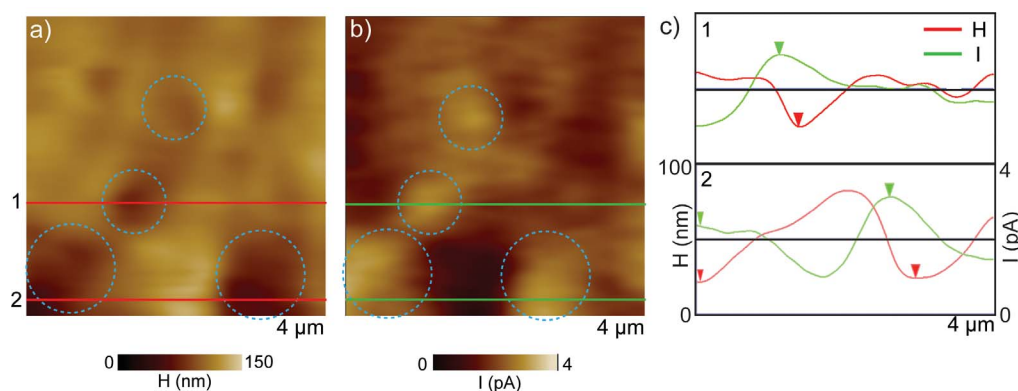


Figure 3 | Simultaneous height (a) and ionic current (b) AFM images of a track etched polycarbonate membrane with nominal pore diameters of $0.8\ \mu\text{m}$. Lighter colors indicate higher currents. As shown in the images and the two cross sections across three pores (c), high correlation is seen between the height and currents at the locations of the three pores indicated by triangles. Red lines are used for height (H) and green for current (I). The scales are the same for both cross sections.

AFM Imaging. A multimode AFM equipped with a Nanoscope IVa controller and a fluid cell (all from Bruker, Santa Barbara, CA) was used to image the AAO membrane in tapping mode. The bath electrode and the tip were connected to a patch clamp amplifier (Dagan, Minneapolis, MN) for simultaneous recording of ionic currents passing through the membrane. The currents were passed into the AFM controller for plotting of the data collected in current recording. Slow scan rates of $0.1\text{--}1\ \text{Hz}$ along with a $20\ \text{Hz}$ lowpass filter were used in all imaging to reduce noise. All electrical recording was performed in a homemade Faraday cage to eliminate noise. Images

were processed following imaging using Nanoscope Analysis Version 1.40 (Bruker, Santa Barbara, CA). All images were flattened and lowpass filtered gaussian filter of 10 pixels in the horizontal and vertical axis.

I–V Curve Recording. Voltages were ramped between $\pm 200\ \text{mV}$ at varying rates using the Nanoscope IVa controller and patch clamp amplifier. An AAO membrane was in place between the tip and the counter electrode. The tungsten probe was withdrawn from the surface to prevent reduction of the current. The current was

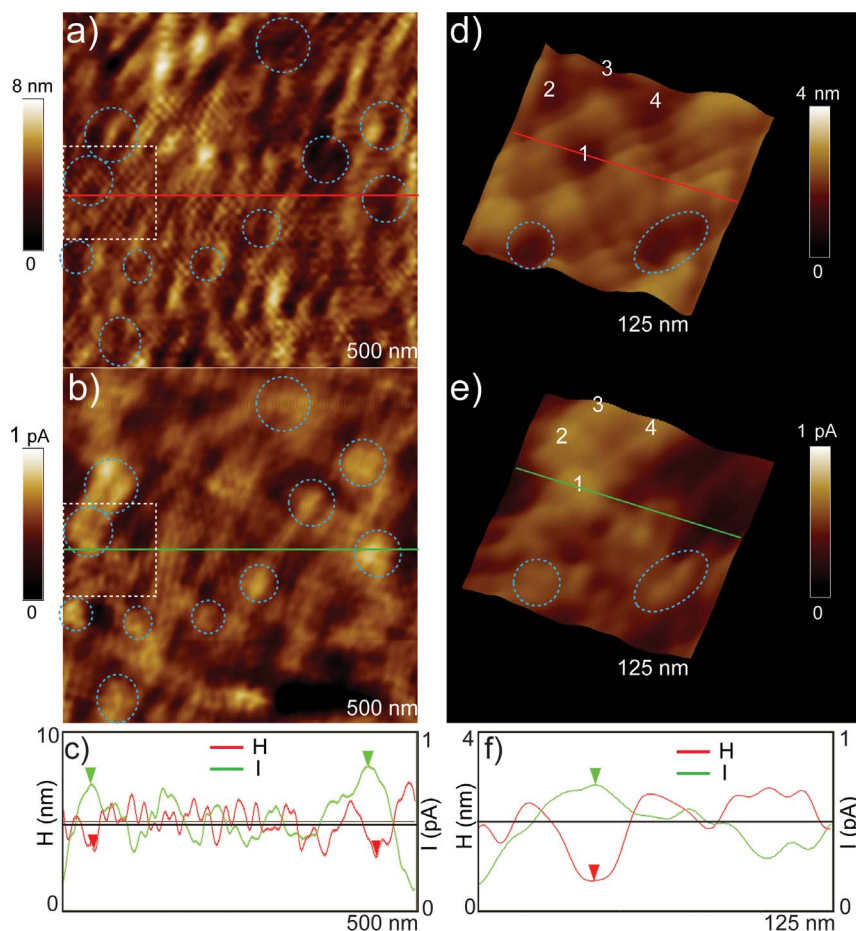


Figure 4 | AFM images of AAO membranes with nominal pore diameters of $18\ \text{nm}$. Simultaneous (a) Height and (b) current images show similar geometry to SEM images and have good correlation with each other. (c) A cross section of the ionic current acquired simultaneously with the height image. Dashed circles indicate pores observed in both images. (d)–(f) similar images and line profiles for the $125 \times 125\ \text{nm}^2$ region indicated by dashed squares in (a)–(b) show that individual pores (marked with numbers 1–4 and dashed circles) are resolved in the height and current images. Red lines are used for height (H) and green for current (I). Images were Fourier filtered to remove noise.



recorded using the setup previously described in the AFM imaging. For electrochemical experiments, $0.1 \text{ M Fe(CN)}_6^{4-}$ was used as the redox active species in 0.1 M phosphate buffer at pH 6.9. Voltammograms were ramped at rates of 0.05 V/s between $\pm 500 \text{ mV}$ against an Ag/AgCl reference/counter electrode utilizing the same setup as the PBS results.

SEM Imaging. Imaging of AAO membranes and tungsten probes was performed on an ultrahigh resolution SEM (FEL, Hillsboro, OR). The membranes were sputter coated in a thin layer ($1\text{--}2 \text{ nm}$) of chromium to make them conducting for imaging.

- Binnig, G., Quate, C. F. & Gerber, C. Atomic force microscope. *Phys. Rev. Lett.* **56**, 930 (1986).
- Hansma, P. K., Drake, B., Marti, O., Gould, S. A. C. & Prater, C. B. The Scanning Ion-Conductance Microscope. *Science* **243**, 641–643 (1989).
- Bard, A. J. *et al.* Chemical imaging of surfaces with the scanning electrochemical microscope. *Science* **254**, 68–74 (1991).
- Böcker, M., Muschter, S., Schmitt, E. K., Steinem, C. & Schäffer, T. E. Imaging and patterning of pore-suspending membranes with scanning ion conductance microscopy. *Langmuir* **25**, 3022–3028 (2009).
- Fan, F.-R. F. & Bard, A. J. Imaging of biological macromolecules on mica in humid air by scanning electrochemical microscopy. *Proc. Natl. Acad. Sci.* **96**, 14222–14227 (1999).
- Korchev, Y. E., Bashford, C. L., Milovanovic, M., Vodyanov, I. & Lab, M. J. Scanning ion conductance microscopy of living cells. *Biophys. J.* **73**, 653–658 (1997).
- Novak, P. *et al.* Nanoscale live-cell imaging using hopping probe ion conductance microscopy. *Nat. Methods* **6**, 279–281 (2009).
- Schäffer, T. E. *et al.* Does abalone nacre form by heteroepitaxial nucleation or by growth through mineral bridges? *Chem. Mat.* **9**, 1731–1740 (1997).
- Shevchuk, A. I. *et al.* Imaging Proteins in Membranes of Living Cells by High-Resolution Scanning Ion Conductance Microscopy. *Angew. Chem. Int. Ed.* **45**, 2212–2216 (2006).
- Proksch, R., Lal, R., Hansma, P. K., Morse, D. & Stucky, G. Imaging the internal and external pore structure of membranes in fluid: TappingMode scanning ion conductance microscopy. *Biophys. J.* **71**, 2155–2157 (1996).
- Quist, A. P. *et al.* Atomic force microscopy imaging and electrical recording of lipid bilayers supported over microfabricated silicon chip nanopores: Lab-on-a-chip system for lipid membranes and ion channels. *Langmuir* **23**, 1375–1380 (2007).
- Macpherson, J. V. & Unwin, P. R. Combined scanning electrochemical-atomic force microscopy. *Anal. Chem.* **72**, 276–285 (2000).
- Macpherson, J. V., Jones, C. E., Barker, A. L. & Unwin, P. R. Electrochemical imaging of diffusion through single nanoscale pores. *Anal. Chem.* **74**, 1841–1848 (2002).
- Gardner, C. E., Unwin, P. R. & Macpherson, J. V. Correlation of membrane structure and transport activity using combined scanning electrochemical-atomic force microscopy. *Electrochem. Commun.* **7**, 612–618 (2005).
- Burt, D. P., Wilson, N. R., Weaver, J. M. R., Dobson, P. S. & Macpherson, J. V. Nanowire probes for high resolution combined scanning electrochemical Microscopy-Atomic force Microscopy. *Nano Lett.* **5**, 639–643 (2005).
- Derylo, M. A., Morton, K. C. & Baker, L. A. Parylene Insulated Probes for Scanning Electrochemical-Atomic Force Microscopy. *Langmuir* **27**, 13925–13930 (2011).
- Wain, A. J., Cox, D., Zhou, S. & Turnbull, A. High-aspect ratio needle probes for combined scanning electrochemical microscopy - Atomic force microscopy. *Electrochem. Commun.* **13**, 78–81 (2011).
- Borzenets, I. V. *et al.* Ultra-sharp metal and nanotube-based probes for applications in scanning microscopy and neural recording. *J. Appl. Phys.* **111**, 074703-074703-074706.
- Bryant, P. J., Kim, H. S., Zheng, Y. C. & Yang, R. Technique for shaping scanning tunneling microscope tips. *Rev. Sci. Instrum.* **58**, 1115 (1987).
- Angle, M. R. & Schaefer, A. T. Neuronal recordings with solid-conductor intracellular nanoelectrodes (SCINs). *PLOS ONE* **7**, e43194 (2012).
- Frederix, P. L. T. M. *et al.* Assessment of insulated conductive cantilevers for biology and electrochemistry. *Nanotechnology* **16**, 997 (2005).
- Schulte, A. & Chow, R. H. A simple method for insulating carbon-fiber microelectrodes using anodic electrophoretic deposition of paint. *Anal. Chem.* **68**, 3054–3058 (1996).
- Abbou, J., Demaille, C., Druet, M. & Moiroux, J. Fabrication of submicrometer-sized gold electrodes of controlled geometry for scanning electrochemical-atomic force microscopy. *Anal. Chem.* **74**, 6355–6363 (2002).
- Chen, C. C., Derylo, M. A. & Baker, L. A. Measurement of ion currents through porous membranes with scanning ion conductance microscopy. *Anal. Chem.* **81**, 4742–4751 (2009).

Acknowledgments

The authors thank Alan Gillman insight in manuscript preparation. This work was supported by grants from the NIH R01DA024871, R01DA025296 R.L. and F31DA034562 B.M. Fellowship support for this work was provided by the NSF for L.S.C.

Author contributions

B.M., F.T.A., L.S.C. and R.L. conceived the idea and prepared the manuscript; B.M., F.T.A. and L.S.C. performed the experiments and analyzed the data.

Additional information

Supplementary information accompanies this paper at <http://www.nature.com/scientificreports>

Competing financial interests: The authors declare no competing financial interests.

How to cite this article: Meckes, B., Arce, F.T., Connolly, L.S. & Lal, R. Insulated Conducting Cantilevered Nanotips and Two-Chamber Recording System for High Resolution Ion Sensing AFM. *Sci. Rep.* **4**, 4454; DOI:10.1038/srep04454 (2014).



This work is licensed under a Creative Commons Attribution-NonCommercial-NoDerivs 3.0 Unported license. To view a copy of this license, visit <http://creativecommons.org/licenses/by-nc-nd/3.0>